Organic & Biomolecular Chemistry

Accepted Manuscript

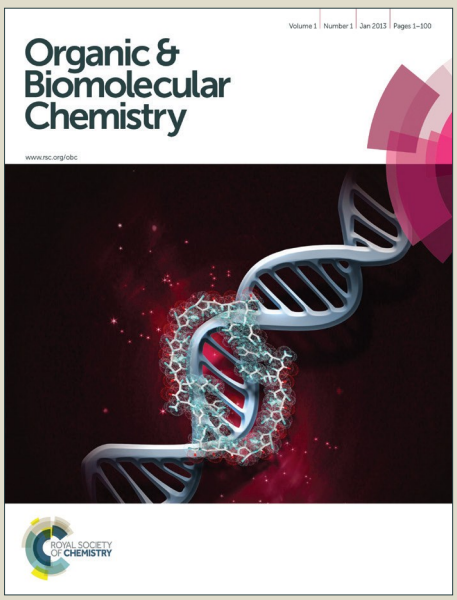

ROYAL SOCIETY OF CHEMISTRY

www.rsc.org/obc

Journal Name

ARTICLE

Optimizing the Lifetimes of Phenoxonium Cations Derived from Vitamin E *via* Structural Modifications

Received 00th January 20xx,
Accepted 00th January 20xx

DOI: 10.1039/x0xx00000x

www.rsc.org/

Yanni Yue,[a] Maria L. Novianti,[a] Malcolm E. Tessensohn,[a] Hajime Hirao[a] and Richard D. Webster[a]*

Systematic synthesis of a number of new phenolic compounds with structures similar to vitamin E led to the identification of several sterically hindered compounds that when electrochemically oxidised in acetonitrile in a $-2e^-/-H^+$ process formed phenoxonium diamagnetic cations that were resistant to hydrolysis reactions. The reactivity of the phenoxonium ions was ascertained by performing cyclic voltammetric scans during the addition of carefully controlled quantities of water into acetonitrile solutions, with the data modelled using digital simulation techniques.

Introduction

Phenoxonium cations are thought to be important intermediates produced during the oxidation of phenols,[1-7] although are usually so short-lived that they are only detected as transients from laser flash photolysis experiments.[8-13] Nevertheless, there exists one class of phenolic compounds based on the 6-chromanol structure (Scheme 1) found in natural vitamin E that form remarkably long-lived phenoxonium ions upon oxidation in acetonitrile or dichloromethane solutions.[14-19] Vitamin E is comprised of a number of structurally related forms which differ in their biological properties. The most biologically active form is termed α-tocopherol which has methyl groups in positions R_1–R_4 while R_5 is comprised of a long ($C_{16}H_{33}$) phytyl chain (Scheme 1).[17] It has been demonstrated that α-tocopherol undergoes a $-2e^-/-H^+$ chemically reversible electrochemical oxidation process to form its associated phenoxonium cation (step 1 in Scheme 1) with the cation surviving for long periods in CH_3CN solutions provided the water content is very low.[16-19] The β-, γ- and δ- forms of the tocopherols, which have lesser amounts of methylation of the aromatic ring, also undergo step 1 in Scheme 1, but their associated phenoxonium ions are much shorter lived because they are considerably more reactive with the trace water present in the solvent and quickly undergo hydrolysis reactions to form first hemiketals (step 2 in Scheme 1), which can ultimately convert into quinones (step 3 in Scheme 1) but in low yields.[16] The phenoxonium cation, hemiketal and quinone shown in Scheme 1 all have significantly different formal electrode potentials, thus the series of reactions can be monitored by voltammetric methods.[18]

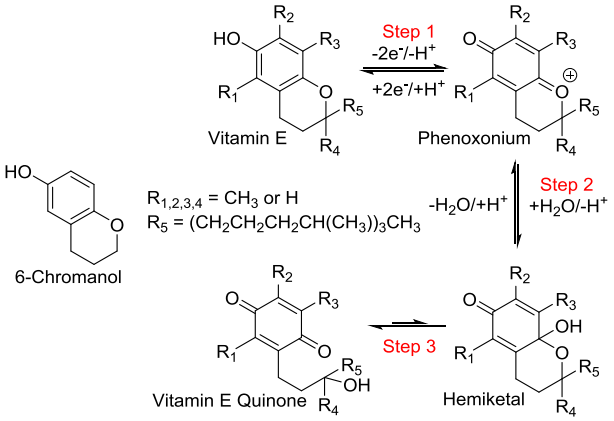

Scheme 1. Electrochemical oxidation mechanism for vitamin E in acetonitrile or dichloromethane solutions containing trace water.

Step 1 in Scheme 1 can be broken down into distinct electron transfer and proton transfer steps as shown in Scheme 2, which is an example of a "proton-coupled electron transfer" (PCET) mechanism. For PCET reactions in general, the combined electron transfer and proton transfer steps can occur in either consecutive (step-wise) or concerted (simultaneous) manners, although it is often very difficult to ascertain the exact mechanism, especially if the proton transfer reaction occurs very quickly.[20-24] For vitamin E, the initial $-2e^-/-H^+$ oxidation is known to occur *via* a consecutive electron and proton transfer mechanism ($-1e^-/-H^+/-1e^-$) progressing through a cation radical and neutral radical (phenoxyl) prior to the formation of the phenoxonium ion (diamagnetic cation) (Scheme 2).[17] Nevertheless, there exists some uncertainty whether the second electron transfer step (step 1c in Scheme 2) occurs heterogeneously at the electrode surface (an ECE mechanism) or whether it occurs homogeneously where a radical cation reacts with a phenoxyl radical to form the phenoxonium cation and the starting material (a disproportionation mechanism).[22]

[a] Division of Chemistry and Biological Chemistry, School of Physical and Mathematical Sciences, Nanyang Technological University, Singapore 637371, Singapore. E-mail: webster@ntu.edu.sg

Electronic Supplementary Information (ESI) available: [full synthetic procedures, compound characterisation data, additional voltammetric scans and computational results]. See DOI: 10.1039/x0xx00000x

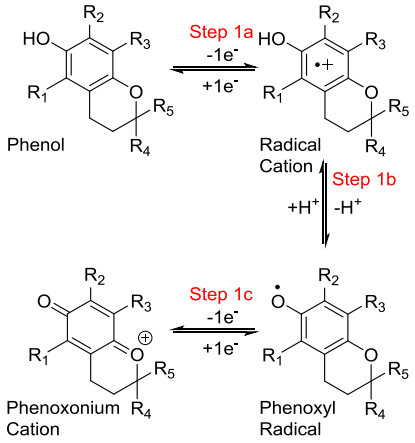

Scheme 2. Electrochemical ECE mechanism for conversion of phenol into a phenoxonium cation.

Most phenolic compounds are thought to undergo the same initial PCET reactions given in Scheme 2 during electrochemical oxidation experiments.[2,3,17] However, a major difference seen with α-tocopherol is that steps 1a-1c are completely chemically reversible such that the starting material can be regenerated on the voltammetric timescale (≤ seconds). Thus, CVs of α-tocopherol in CH_3CN or CH_2Cl_2 contain both a forward oxidation peak and a reverse reduction peak when the scan direction is reversed. This is in contrast to what is generally observed for the voltammetric behaviour of phenols where only a forward peak is seen (corresponding to an initial $-2e^-/-H^+$ oxidation) but no corresponding reduction peak is observed even at very fast scan rates due to the high reactivity of the phenoxonium cations derived from most phenolic compounds.[2,3] An exception is seen in CVs of phenols that can undergo strong intramolecular hydrogen–bonding interactions through the phenolic hydrogen atom, but these are oxidised in a chemically reversible $-1e^-$ process.[20,22]

Due to the unusually long lifetime of the phenoxonium cation of α-tocopherol compared to other phenols (and even to other closely related tocopherols), it has been proposed that the phenoxonium cation may have importance in α-tocopherol's biological functions.[16,17] This proposal was partly based on the disagreements in the literature about vitamin E's true biological function; some groups argue that it is only an antioxidant,[25] while other groups argue for additional non-antioxidant roles such as a cellular signaling molecule.[26] While the antioxidant mechanisms are well established and can be experimentally tested by examining biological markers (metabolites produced via free radical reactions),[27,28] for the non-antioxidant case there are no detailed mechanisms currently in existence. It is unlikely that the phenoxonium cation has any role in the antioxidant mechanisms but it may conceivably play a role in the non-antioxidant cases (should they occur). Chemically reversible PCET reactions are not without precedent in the biological functions of other lipophilic vitamins; for example, vitamin K_1 and vitamin B_2 both undergo two-electron two-proton reduction mechanisms.[29,30] However, the existence of the phenoxonium cation is very difficult to test for under real biological conditions. Therefore, the long-term goal of this work was to synthesise modified compounds based on α-tocopherol's chromanol structure that form even longer-lived phenoxonium cations upon oxidation. Future work will then be directed at examining the biological properties of the modified compounds.

Results and Discussion

This study was directed towards investigating whether modifying the structure of α-tocopherol could make the associated phenoxonium cation formed by the voltammetrically induced $-2e^-/-H^+$ transfer more long-lived in the presence of trace water, by slowing down the hydrolysis reaction in step 2 in Scheme 1. Since the reaction of the phenoxonium cation with water occurs at the carbon in the *para* position to the carbonyl group, it was thought that placing a bulky group adjacent to this carbon (i.e. substituting R_3) would slow down the hydrolysis reaction due to steric blocking. A number of new phenolic compounds were synthesized and voltammetrically tested in acetonitrile containing varying amounts of water (full synthetic procedures are provided in the Electronic Supplementary Information, ESI).

Figure 1 shows the cyclic voltammograms recorded in CH_3CN of the α-tocopherol model compound (containing a methyl group at R_5) [(CH_3)α-TOH] (black) as well as all of the synthesised compounds (red or blue) at a scan rate of 0.1 V s^{-1} and with relatively low amounts of trace water. It has been found that replacing the phytyl chain (R_5) that is present in the natural compound with a methyl group does not change the voltammetric response;[17,32] therefore, to decrease the complexity of the initial synthesis procedures, the methyl containing analogues (at R_5) were mainly prepared.

The initial amount of water was controlled by drying the solvent/electrolyte over 3 Å molecular sieves in a previously described procedure.[31] The water inside the electrochemical cell was measured using a Karl Fischer coulometric titrator that was placed inside a humidity chamber. However, it is difficult to control the exact amount of residual water in the electrochemical solution, so the starting trace amount is slightly different in each case. The starting water content was approximately 10 – 25 mM and the water content was successively increased and cyclic voltammograms (CVs) were recorded.

The CV for the α-tocopherol model compound [(CH_3)α-TOH] shows a forward oxidation peak (E_p^{ox}) at +0.4 V *vs.* Fc/Fc^+ (Fc = ferroene) and a reverse reduction peak (E_p^{red}) at +0.2 V *vs.* Fc/Fc^+ (black trace in Figure 1). The forward process is known to involve the $-2e^-/-H^+$ step 1 reaction in Scheme 1 to form the phenoxonium cation while the reduction process that is seen when the scan direction is reversed involves the transformation of the phenoxonium cation back to the starting material.[16-19,32] The reason that there is a relatively wide separation between the forward and reverse peaks is because the electron transfers occur in two one-electron steps with each step having a different formal electrode potential (steps 1a and 1c in Scheme 2).[16-19,32]

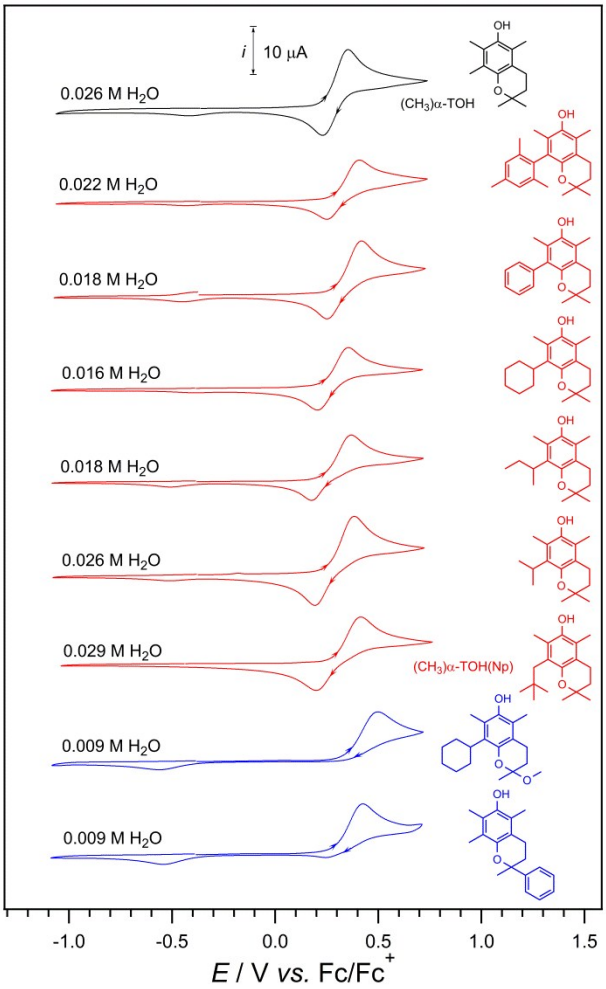

Figure 1. CVs of 2 mM of analytes recorded in CH_3CN containing 0.2 M Bu_4NPF_6 at a 1 mm diameter circular planar Pt electrode at 22 ± 2 °C at a scan rate of 0.1 V s^{-1} at the specified concentration of trace water.

The compounds drawn in red in Figure 1 all have the methyl group at R_3 that is present in natural α-tocopherol replaced with a more bulky hydrocarbon. The CVs of the molecules drawn in red appear very similar to that of (CH_3)α-TOH, showing an oxidation peak on the forward scan and a reduction peak when the scan direction is reversed, all occurring at similar potentials. Based on the close similarity between the CV of the α-tocopherol model compound and the CVs of the molecules drawn in red, it can be proposed that they all undergo the same oxidation mechanism and that their phenoxonium cations can be reversibly reduced back to the starting materials on the CV timescale. The majority of the synthesised compounds were designed with bulky hydrocarbon substituents at R_3 in order to provide steric hindrance from nucleophilic attack at the aromatic ether carbon of the phenoxonium cation. However, it is also important for the substituents at R_3 not to strongly alter the electronic energy levels of the cation (such as would occur with highly electron-donating or withdrawing groups) which are also likely to be highly important in controlling the reactivity of the formed cations.

The two compounds drawn in blue in Figure 1 have the methyl group at R_4 replaced with either a methoxy or phenyl group. The CVs for both of these compounds show a forward oxidation peak with only a very small or no reverse reduction peak (close to the main oxidation process) when the scan direction is reversed, indicating that the phenoxonium cations of these compounds are relatively short-lived. The reason for the lack of chemical reversibility is because it has been shown (*via* ^{13}C NMR spectroscopy and density functional theory calculations)[32] that the phenoxonium cation of α-tocopherol has a surprisingly large amount of positive charge localized on the sp^3 carbon in the chromanol ring (C_9), thus substitution of R_4 with an electron-donating or withdrawing group affects the electronic charge distribution and increases the reactivity of the cation. Therefore, in order to provide the longest lifetimes of the diamagnetic cations derived from the oxidation of compounds with structures similar to α-tocopherol, it is preferable if substituents R_4 and R_5 are based solely on simple alkyl chains.[18]

The CVs in Figure 1 only allow for a comparison of the compounds at relatively low water content, but can be interpreted as indicating that the phenoxonium cations of the compounds drawn in red are equally as resistant to hydrolysis as the α-tocopherol model compound. For the next stage of the analysis, controlled amounts of water were added to individual acetonitrile solutions containing the compounds that showed both forward oxidation and reverse reduction processes at +0.4 and +0.2 V vs. Fc/Fc+, respectively, and CVs were recorded at a fixed scan rate of 0.1 V s^{-1}. It was reasoned that the reverse reduction peak that is detected after first oxidising the starting material would become smaller if the oxidised compound reacts with excess water (according to step 2 in Scheme 1), thus a comparison of all the compounds at similar water contents would give a relative measure of which phenoxonium cations were the most resistant to hydrolysis.

The left hand side voltammograms in Figure 2 show the CVs that were obtained when water was added to the solution containing the α-tocopherol model compound, (CH_3)α-TOH. It can be seen in Figure 2 that as water is progressively added to a solution containing (CH_3)α-TOH, the reverse reduction peak that occurs at approximately +0.2 *vs.* Fc/Fc^+ becomes smaller in comparison with the forward oxidation process at +0.4 V *vs.* Fc/Fc^+. At a water content of approximately 0.2 M, the reverse reduction peak at +0.2 vs. Fc/Fc^+ can barely be detected indicating that the phenoxonium cation is reacting with the large excess of water according to step 2 in Scheme 1. Furthermore, the reduction process that occurs at ~–0.5 V *vs.* Fc/Fc^+ (which is only evident if the potential is first applied in the positive direction so as to oxidise the starting material) becomes larger as more water is added to solution. This process at ~–0.5 V *vs.* Fc/Fc^+ has been assigned in previous studies as associated with the reduction of the hemiketal that forms according to step 2 in Scheme 1 (and is also clearly seen in the CVs of the compounds drawn in blue in Figure 1).[18]

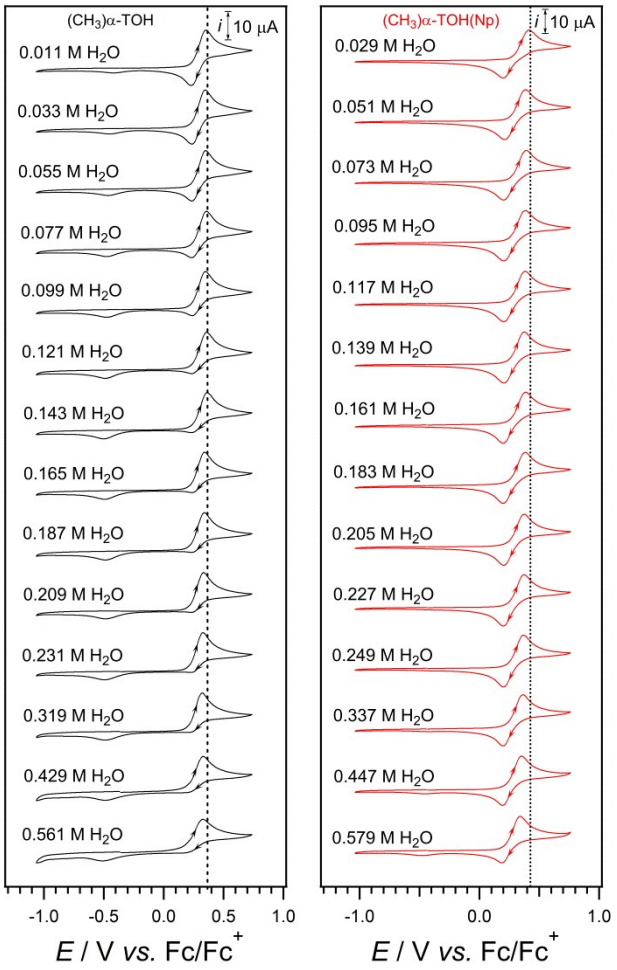

Figure 2. CVs of 2 mM of the α-tocopherol model compound [(CH_3)α-TOH] and neopentyl derivative [(CH_3)α-TOH(Np)] in CH_3CN containing 0.2 M Bu_4NPF_6 at a 1 mm diameter circular planar Pt electrode at 22 ± 2 °C at a scan rate of 0.1 V s^{-1} at the specified concentration of water.

It can also be observed in Figure 2 that the oxidation peak shifts to less positive potentials as water is added to the solvent. This phenomenon can be explained based on a hydrogen-bonding mechanism that occurs between the phenolic hydrogen in α-tocopherol (and for phenols in general)[22,23,33-36] and H_2O molecules.[19] Because the peak potentials shift with the amount of trace water and because the voltammetric processes involve two one-electron transfers interspaced with a chemical step, there is not a simple relationship between the peak potentials and the formal electrode potentials. Instead the formal potentials need to be estimated by digital simulation of the entire voltammetric waves.[19]

The right hand side voltammograms in Figure 2 show CV data that were obtained for the neopentyl R_3 substituted compound [(CH_3)α-TOH(Np)] as water was added to the solvent. It can be observed that for the neopentyl derivative, the amount of water that needed to be added in order to lose the reverse reduction peak was substantially greater than that observed for (CH_3)α-TOH (compare left and right hand side CVs in Figures 2). Therefore, it can be concluded that the phenoxonium cation of (CH_3)α-TOH(Np) is less reactive towards water than the phenoxonium cation of (CH_3)α-TOH. Similar CV experiments in the presence of varying concentrations of water were performed for the other compounds shown in red in Figure 1 (see Figures S1 – S5 in the ESI) and it was found that the neopentyl derivative was the best performing (in terms of less reactivity with water) although all of the other compounds also showed improvements over the α-tocopherol model compound.

It can be observed in Figure 2 that the E_p^{ox}-values for [(CH_3)α-TOH(Np)] also shift to less positive potentials as water is added to the solution, and to a greater degree than for [(CH_3)α-TOH]. The shifts have been attributed to hydrogen-bonding between water molecules and the phenolic hydrogen atom,[19] which implies that there is more hydrogen-bonding occurring with the neopentyl derivative. The exact reason for this difference between the two compounds has not been ascertained, but it clearly does not affect the lifetime of the phenoxonium cation of the neopentyl derivative, as the hydrogen-bonding is not occurring in the region of the ether oxygen. At very high concentrations of water it is also observed that the peak associated with the reduction of the hemiketal at ~–0.5 V *vs*. Fc/Fc^+ is also detected for [(CH_3)α-TOH(Np)] indicating that the hydrolysis reaction still occurs to some degree.

Further evidence for the persistent existence of the phenoxonium cation of (CH_3)α-TOH(Np) came from *in situ* electrochemical-UV-vis spectroscopy, which led to the detection of an oxidised product with a spectrum the same as that obtained during the oxidation of (CH_3)α-TOH, which was previously proven to be that of the phenoxonium cation (Figure 3).[17]

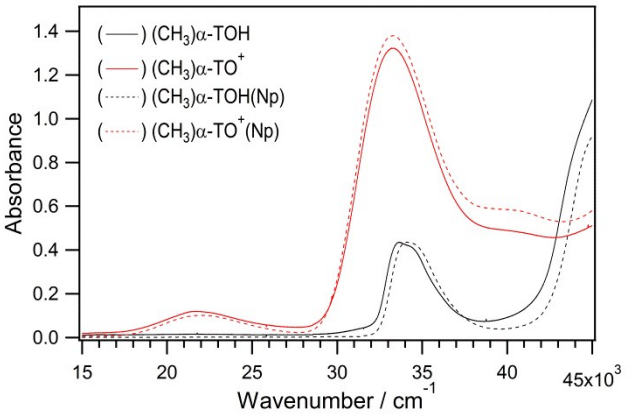

Figure 3. In situ electrochemical-UV-vis spectra obtained before and after the two-electron one-proton oxidation of 1 mM (CH_3)α-TOH or 1 mM (CH_3)α-TOH(Np) in CH_3CN or CH_2Cl_2 at 243 K with 0.5 M Bu_4NPF_6. Data for (CH_3)α-TOH/(CH_3)α-TO^+ were modified from reference 16.

Molecular geometry optimizations based on density functional theory (DFT) calculations performed for $(CH_3)\alpha$-TOH and $(CH_3)\alpha$-TOH(Np) and their oxidised forms (in the gas phase as well as in acetonitrile) indicated that the phenoxonium cations of both compounds had structures with very similar bond lengths (Table S1 in the ESI). The similarity in structural arrangements and observed oxidation peak potentials indicate that the change from the methyl to the neopentyl group at R_3 has little effect on the electron configuration of the neutral and cationic compounds. Therefore, the increase in the lifetime of the phenoxonium cation of $(CH_3)\alpha$-TOH(Np) is due to the steric effects of the neopentyl group reducing the rate of hydrolysis. The increase in bulkiness at R_3 is illustrated diagrammatically in Figure S7 in the ESI.

In order to quantitatively determine the reactivity of the phenoxonium cation of $(CH_3)\alpha$-TOH(Np) with H_2O compared to the reactivity of the cation of $(CH_3)\alpha$-TOH, the voltammetric data were modelled using digital simulation techniques. The full mechanism, electrochemical and kinetic simulation parameters and the CV data are provided in Scheme 3, Tables 1 and 2 and Figure 4, respectively. Previous simulation studies had allowed an estimate of the rate of hydrolysis for the phenoxonium cation of $(CH_3)\alpha$-TOH (Eq 2 in Scheme 3) of 11 L mol^{-1} s^{-1}.[19] In the present study, the hydrolysis reaction rate for the phenoxonium cation of $(CH_3)\alpha$-TOH(Np) was estimated to be 0.5 L mol^{-1} s^{-1}, which is approximately 20 times slower. The simulation studies required the experimental data to be obtained at relatively high water concentrations of 0.7 M in order to be able to observe the hydrolysis reaction being outrun as the voltammetric scan rates were increased from 0.1 – 20 V s^{-1} (Figure 4).

The simulation parameters used for $(CH_3)\alpha$-TOH(Np) were very similar to those previously used for $(CH_3)\alpha$-TOH (see Tables 1 and 2) except for the hydrolysis step (Eq 2), which supports the overall mechanism between the compounds being identical except for the rate of the hydrolysis reaction. The hemiketal in Scheme 3 was invoked as an intermediate because previous voltammetric and solution phase infrared experiments on $(CH_3)\alpha$-TOH led to the identification of an oxidised species that formed after the phenoxonium cation but before the quinone.[18] Because it was possible to reduce the intermediate back to the starting material it was reasoned that a ring open form (such as a quinone) was less likely. Evidence for the hemiketal is also present in the CVs of the neopentyl and other derivatives shown in Figure 1, in the form of the reduction process that occurs on the reverse scan at approximately –0.5 V *vs.* Fc/Fc^+ after first oxidising the starting materials.

A direct reaction of H_2O at the sp^3 carbon (C_9) or simultaneous cleavage of the sp^3 carbon-oxygen bond is also possible and cannot be ruled out based on the present experimental data. Unlike the DFT calculations, the electrochemical simulations are "blind" to the exact chemical structures of the compounds involved in the reaction. Therefore, the forward rate constant for Eq 2 (the reaction of the phenoxonium cation with water) remains that same regardless of the exact identity of the species formed by the reaction. Furthermore, the following chemical steps (Eqs 3, 4 and 5) are only represented in the simulations as the small peak that is detected on the reverse scan at ~-0.5 V vs. Fc/Fc^+.

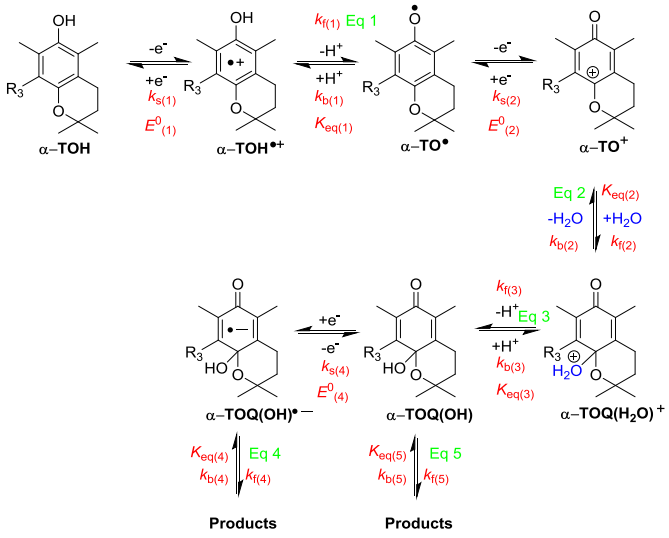

Scheme 3. Full electrochemical oxidation mechanism used in digital simulations.

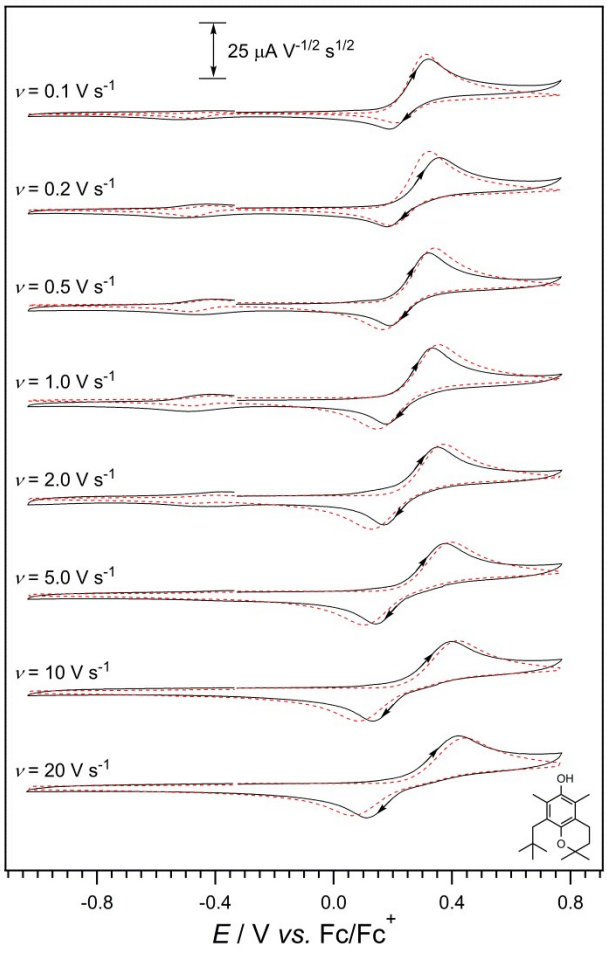

Figure 4. (Black solid lines) CVs of 2 mM R_3 neopentyl substituted compound in CH_3CN containing 0.2 M Bu_4NPF_6 and 0.7 M H_2O at a 1 mm diameter circular planar Pt electrode at 22 ± 2 °C at variable scan rates. (Red dashed lines) Digitally simulated voltammograms based on the mechanism in Scheme 3 and the data in Tables 1 and 2.

Table 1. Electrochemical parameters used in the digital simulations of CV[a] data for the α-tocopherol model compound [(CH_3)α-TOH] and its neopentyl derivative [(CH_3)α-TOH(Np)], and based on the mechanism in Scheme 3.

Compound	$E^0_{f(1)}$ / V *vs.* Fc/Fc^+	$k_{s(1)}$ / cm s^{-1}	$E^0_{f(2)}$ / V *vs.* Fc/Fc^+	$k_{s(1)}$ / cm s^{-1}	$E^0_{f(3)}$ / V *vs.* Fc/Fc^+	$k_{s(1)}$ / cm s^{-1}	[c]*D* / cm^2 s^{-1}
(CH_3)α-TOH[b]	0.5 (±0.1)	0.1 – 0.3	0.1 (±0.1)	0.1 – 0.3	-0.3 (±0.2)	0.1 – 0.3	2.0×10^{-5}
(CH_3)α-TOH(Np)	0.5 (±0.1)	0.1 – 0.3	0.1 (±0.1)	0.1 – 0.3	-0.3 (±0.2)	0.1 – 0.3	1.5×10^{-5}

[a]CV data recorded in in CH_3CN containing H_2O with 0.2 M *n*-Bu_4NPF_6 as the supporting electrolyte at a 1 mm diameter planar circular Pt electrode at 22 (±2) °C, at scan rates between 0.1 – 20 V s^{-1}. [b]Values for (CH_3)α-TOH are taken from reference 19. [c]Diffusion coefficient values for the starting material and all oxidised forms. *D*-values for H_2O and H^+ were set at 4.0×10^{-5} cm^2 s^{-1}.

Table 2. Kinetic parameters used in the digital simulations of CV[a] data for the α-tocopherol model compound [(CH_3)α-TOH] and its neopentyl derivative [(CH_3)α-TOH(Np)], and based on the mechanism in Scheme 3.

Compound	Kinetic Parameters[c]	Eq 1	Eq 2	Eq 3	Eq 4	Eq 5
(CH_3)α-TOH[b]	K_{eq}	1.4×10^{-4}	1	1.0×10^{3}	1.0×10^{3}	1.0×10^{3}
	k_f	3.0×10^{4}	11 ± 4	3.0×10^{4}	1	1
	k_b	2.5×10^{8}	11 ± 4	30	1.0×10^{-3}	1.0×10^{-3}
(CH_3)α-TOH(Np)	K_{eq}	1.4×10^{-4}	1	1.0×10^{3}	1.0×10^{3}	1.0×10^{3}
	k_f	3.0×10^{4}	0.5 ± 0.2	3.0×10^{4}	1	1
	k_b	2.5×10^{8}	0.5 ± 0.2	30	1.0×10^{-3}	1.0×10^{-3}

[a]CV data recorded in in CH_3CN containing H_2O with 0.2 M *n*-Bu_4NPF_6 as the supporting electrolyte at a 1 mm diameter planar circular Pt electrode at 22 (±2) °C, at scan rates between 0.1 – 20 V s^{-1}. [b]Values for (CH_3)α-TOH are taken from reference 19. [c]Homogeneous rate constants for the forward (k_f) and back (k_b) reactions have units of s^{-1} and L mol^{-1} s^{-1} for first- and second-order reactions, respectively.

The Mulliken and natural bond orbital calculated atomic charges obtained from DFT calculations indicated that there were relatively high positive charges on the two carbon atoms forming the ether linkage (C_1 and C_9) in the phenoxonium cation (Tables S2 and S3 in the ESI). These high charges do support the conclusion that further reactions with H_2O will occur at either C_1 or C_9. However, despite the phenoxonium cation forming in 100% yield following the chemical or electrochemical oxidation, attempts to characterise the long-term products of further reactions with water (added to acetonitrile) have resulted in the formation of a large number of products which have not been isolated and identified to date.[18]

Experimental

Cyclic voltammetry

Cyclic voltammetry experiments were conducted with a computer-controlled Eco Chemie Autolab PGSTAT302N potentiostat in a three-electrode cell where a 1 mm diameter planar platinum (Pt) disk (Cypress Systems) working electrode was used together with a platinum wire (Metrohm) auxiliary electrode. A platinum wire (Metrohm) reference electrode was used in the presence of 3 Å molecular sieves for the experiments under ultra-dry conditions whereas a silver wire (Cypress Systems) miniature reference electrode connected to the test solution *via* a salt bridge containing 0.5 M *n*-Bu_4NPF_6 in CH_3CN was employed in all other experiments. The internal filling solution of the liquid-junction reference electrode was freshly prepared before each experiment to reduce the amount of water that it contributed to the analyte solution.

Digital simulations of the CV data were performed using the DigiElch software package, whose theoretical basis has been described extensively in literature reports.[37-42] Simulations of CVs were performed by a trial and error method successively refining the simulation parameters until the simulated voltammograms closely matched the experimental curves. The formal potentials (E^0_f) given in Table 1 needed to be obtained via the simulations since they could only be measured approximately from the experimental data, since the voltammetric peaks were shifted from the E^0_f–values due to the proton transfer accompanying the electron transfer steps. For each simulation, all the parameters in Tables 1 and 2 were used. However, the effects of the different rate and equilibrium constants were not necessarily noticeable at all of the scan rates. Therefore, in order to ensure that the optimal kinetic and electrochemical parameters were obtained, the one set of parameters given in Tables 1 and 2 had to match all the experimental data over a range of scan rates. It was found that most of the simulation parameters were the same as previously found for (CH_3)α-TOH except for the rate constants for the hydrolysis step (Eq 2), and the diffusion coefficients (which were smaller for the bulky neopentyl derivative).

Karl Fischer Coulometric Titrations

Karl-Fischer titrations were performed with a Mettler Toledo DL32 coulometer using (Riedel-deHaën) HYDRANAL®-Coulomat AG and HYDRANAL®-Coulomat CG as the anolyte and catholyte, respectively. The coulometer was allowed to stabilize until a steady drift value close to 0 μg min^{-1} of water was achieved. Constant humidity (30%) measurements were carried out in a (122 cm × 61 cm × 61 cm) humidity control box using a dry nitrogen gas purge system from Coy Laboratory Products Inc. Glass vacuum syringes were used to inject approximately 1 mL aliquots of the electrochemical solutions, *via* a silicon/Teflon septum; the individual measurements were found to conclude within one minute, thereby indicating that the drift from atmospheric water was insignificant.

UV-vis spectroscopy

In situ UV-vis spectra were obtained with a Perkin-Elmer Lambda 750 spectrophotometer in an optically semi-transparent thin layer electrochemical (OSTLE) cell (pathlength = 0.05 cm) using a Pt mesh working electrode.[43]

Computational Studies

The molecular geometries were drawn using GaussView5 and optimized with the B3LYP hybrid density functional[44] with the 6-311+G(2df,p) Pople-style Gaussian basis set[45,46] with solvation effects from CH_3CN taken into account within the Gaussian 09 default suite of programs.[47] The final geometries of the compounds were verified to stay at true energy minima by performing frequency calculations at the B3LYP/6-311+G(2df,p) level that yielded no imaginary frequencies. Zero-point energies were scaled by a factor of 0.9889.[48] Mulliken and natural bond orbital (NBO) calculated atomic charges were obtained from DFT calculations at the B3LYP/6-31(G) level of theory.

Conclusions

Placing bulky hydrocarbon substituents in the R_3 position in the aromatic ring of compounds based on the structure of α-tocopherol aids in increasing the lifetime of their associated phenoxonium cations by providing steric hindrance from nucleophilic attack by water. To date, the best compound that has been synthesised is the neopentyl derivative whose phenoxonium cation is significantly more long-lived than that of α-tocopherol. Considering that phenoxonium cations are usually extremely reactive with even trace nucleophiles, the improved lifetime (up to 20 times longer) compared to the naturally occurring compound indicates that the substituted derivatives do represent the most long-lived phenoxonium cations known to date. Future experiments will investigate whether these modified forms of α-tocopherol have a purpose in any of the non-antioxidant functions of vitamin E,[49] which can be tested via the synthesis of more biological compatible versions of the compounds in red in Figure 1 which have a phytyl chain in the R_5 position.

Acknowledgements

This work was supported by an A*Star SERC Public Sector Funding (PSF) Grant (112 120 2006).

Notes and references

1 K. Yoshida in Electrooxidation in Organic Chemistry: The Role of Cation Radicals as Synthetic Intermediates, Wiley, New York, 1983, pp. 174–186.
2 O. Hammerich and B. Svensmark in Organic Electrochemistry, 3rd ed.; H. Lund, M. M. Baizer, Eds.; Marcel Dekker, New York, 1991, Chapter 16.
3 A. Rieker, R. Beisswenger and K. Regier, Tetrahedron 1991, 47, 645–654.
4 J. C. Green and T. R. R. Pettus, *J. Am. Chem. Soc.* 2011, **133**, 1603–1608.
5 C. Gaeta, C. Talotta and P. J. Neri, *Incl. Phenom. Macro.* 2014, **79**, 23–46.
6 S. Kundu, E. Miceli, E. R. Farquhar and K. Ray, *Dalton Trans.* 2014, **43**, 4264–4267.
7 T. Jähnert, M. D. Hager and U. S. Schubert, *J. Mater. Chem. A.* 2014, **2**, 15234–15251.
8 M. Novak, S. A. Glover, *J. Am. Chem. Soc.* **2004**, *126*, 7748–7749.
9 Y.-T. Wang, J. Wang, M. S. Platz and M. Novak, *J. Am. Chem. Soc.* 2007, **129**, 14566–14567.
10 Y.-T. Wang, K. J. Jin, S. H. Leopold, J. Wang, H.-L. Peng, M. S. Platz, J. Xue, D. L. Phillips, S. A. Glover and M. Novak, *J. Am. Chem. Soc.* 2008, **130**, 16021–16030.
11 P. J. Hanway and A. H. Winter, *J. Am. Chem. Soc.* 2011, **133**, 5086–5093.
12 P. J. Hanway, J. Xue, U. Bhattacharjee, M. J. Milot, R. Zhu, D. L. Phillips and A. H. Winter, *J. Am. Chem. Soc.* 2013, **135**, 9078–9082.
13 M.-D. Li, P. J. Hanway, T. R. Albright, A. H. Winter and D. L. Philips, *J. Am. Chem. Soc.* 2014, **136**, 12364–12370.
14 M. F. Marcus and M. D. Hawley, *Biochim. Biophys. Acta* 1970, **201**, 1–8.
15 U. Svanholm, K. Bechgaard and V. D. Parker, *J. Am. Chem. Soc.* 1974, **96**, 2409–2413.
16 G. J. Wilson, C. Y. Lin and R. D. Webster, *J. Phys. Chem. B* 2006, **110**, 11540–11548.
17 R. D. Webster, *Acc. Chem. Res.* 2007, **40**, 251–257.
18 H. M. Peng and R. D. Webster, *J. Org. Chem.* 2008, **73**, 2169–2175.
19 Y. S. Tan, S. S. Chen, W. M. Hong, J. M. Kan, E. S. H. Kwek, S. Y. Lim, Z. H. Lim, M. E. Tessensohn, Y. Zhang and R. D. Webster, *Phys. Chem. Chem. Phys.* 2011, **13**, 12745–12754.
20 C. Costentin, M. Robert and J.-M. Savéant, *J. Am. Chem. Soc.* 2006, **128**, 4552–4553.
21 M. H. V. Huynh and T. J. Meyer, *Chem. Rev.* 2007, **107**, 5004–5064.
22 C. Costentin, *Chem. Rev.* 2008, **108**, 2145–2179.
23 C. Costentin, M. Robert and J.-M. Savéant, *Acc. Chem. Res.* **2010**, *43*, 1019–1029.
24 J. M. Mayer, *Acc. Chem. Res.* 2011, **44**, 36–46.
25 M. G. Taber and J. Atkinson, *Free Rad. Bio. Med.* 2007, **43,** 4–15.
26 A. Azzi, *Free Radical Biol. Med.* 2007, **43**, 16–21.
27 G. W. Burton and K. U. Ingold, *Acc. Chem. Res.* 1986, **19**, 194–201.
28 E. Niki and N. Noguchi, *Acc. Chem. Res.* 2004, **37**, 45–51.
29 R. D. Webster, *Chem. Rec.* 2012, **12**, 188–200.
30 S. L. J. Tan and R. D. Webster, *J. Am. Chem. Soc.* 2012, **134**, 5954–5964.
31 Y. Hui and R. D. Webster, *Anal. Chem.* 2011, **83**, 976–981.
32 S. B. Lee, C. Y. Lin, P. M. W. Gill and R. D. Webster, *J. Org. Chem.* 2005, **70**, 10466–10473.
33 C. Costentin, C. Louault, M. Robert and J.-M. Savéant, *J. Am. Chem. Soc.* 2008, **130**, 15817–15819.
34 C. Costentin, C. Louault, M. Robert and J.-M. Savéant, *PNAS.* 2009, **106**, 18143–18148.
35 C. Costentin, M. Robert and J.-M. Savéant, *Phys. Chem. Chem. Phys.* **2010**, *12*, 11179–11190.
36 J. Bonin, C. Costentin, C. Louault, M. Robert and J.-M. Savéant, *J. Am. Chem. Soc.* **2011**, *133*, 6668–6674.
37 M. Rudolph, *J. Electroanal. Chem.* 2003, **543**, 23–39.
38 M. Rudolph, *J. Electroanal. Chem.* 2003, **558**, 171–176.
39 M. Rudolph, *J. Electroanal. Chem.* 2004, **571**, 289–307.
40 M. Rudolph, *J. Comput. Chem.* 2005, **26**, 619–632.
41 M. Rudolph, *J. Comput. Chem.* 2005, **26**, 633–641.
42 M. Rudolph, *J. Comput. Chem.* 2005, **26**, 1193–1204.

43 R. D. Webster, G. A. Heath and A. M. Bond, *J. Chem. Soc., Dalton Trans.* 2001, 3189–3195.
44 A. D. Becke, *J. Chem. Phys.* 1993, 98, 5648–5652.
45 A. D. McLean and G. S. Chandler, *J. Chem. Phys.* 1980, **72**, 5639–5648.
46 R. Krishnan, J. S. Bailey, R. Seeger and J. A. Pople, *J. Chem. Phys.* 1980, **72**, 650–654.
47 M. J. Frisch, G. W. Trucks, H. B. Schlegel, G. E. Scuseria, M. A. Robb, J. R. Cheeseman, G. Scalmani, V. Barone, B. Mennucci, G. A. Petersson, H. Nakatsuji, M. Caricato, X. Li, H. P. Hratchian, A. F. Izmaylov, J. Bloino, G. Zheng, J. L. Sonnenberg, M. Hada, M. Ehara, K. Toyota, R. Fukuda, J. Hasegawa, M. Ishida, T. Nakajima, Y. Honda, O. Kitao, H. Nakai, T. Vreven, J. A. Montgomery, Jr., J. E. Peralta, F. Ogliaro, M. Bearpark, J. J. Heyd, E. Brothers, K. N. Kudin, V. N. Staroverov, R. Kobayashi, J. Normand, K. Raghavachari, A. Rendell, J. C. Burant, S. S. Iyengar, J. Tomasi, M. Cossi, N. Rega, N. J. Millam, M. Klene, J. E. Knox, J. B. Cross, V. Bakken, C. Adamo, J. Jaramillo, R. Gomperts, R. E. Stratmann, O. Yazyev, A. J. Austin, R. Cammi, C. Pomelli, J. W. Ochterski, R. L. Martin, K. Morokuma, V. G. Zakrzewski, G. A. Voth, P. Salvador, J. J. Dannenberg, S. Dapprich, A. D. Daniels, Ö. Farkas, J. B. Foresman, J. V. Ortiz, J. Cioslowski and D. J. Fox, *Gaussian 09*, Revision B.01, Gaussian, Inc., Wallingford CT, **2010**.
48 J. P. Merrick, D. Moran and L. Radom, *J. Phys. Chem. A* 2007, **111**, 11683–11700.
49 J.-M. Zingg and A. Azzi, *Curr. Med. Chem.* 2004, **11**, 1113–1133.